A comparative study on borehole heat exchanger size for direct ground coupled cooling systems using active chilled beams and TABS

Energy & Buildings 240 (2021) 110874

Contents lists available at ScienceDirect

Energy & Buildings

journal homepage: www.elsevier.com/locate/enb

A comparative study on borehole heat exchanger size for direct ground coupled cooling systems using active chilled beams and TABS

Taha Arghand *, Saqib Javed, Anders Trüschel, Jan-Olof Dalenbäck

Division of Building Services Engineering, Department of Architecture and Civil Engineering, Chalmers University of Technology, 412 96 Gothenburg, Sweden

ARTICLE INFO

Article history:
Received 9 August 2020
Revised 18 February 2021
Accepted 1 March 2021
Available online 9 March 2021

Keywords:
Direct ground cooling
Borehole heat exchanger
Active chilled beam
Free cooling
GeoTABS
Geocooling

ABSTRACT

Direct ground cooling is a method for cooling buildings whereby free cooling is provided by circulating water through borehole heat exchangers (BHEs). Since no refrigeration cooling is involved, supply water temperature to the building's cooling system is dependent mainly on BHE sizing. This study investigates the sizing of BHEs for direct ground cooling systems, with a particular focus on the influence of terminal unit types and their operating strategies. Experimental results using a direct ground-coupled active chilled beam (ACB) system are used to develop a simulation model for an office building. The model is also modified for thermally activated building systems (TABS). The simulation results show that using TABS instead of ACBs for a similar BHE reduced the ground peak hourly loads, resulting in a lower borehole outlet temperature. Resizing BHE depth to reach similar maximum borehole outlet temperatures according to the actual heat extraction rate from the cooling systems resulted in a significantly shorter BHE depth with TABS compared to ACBs. However, indoor temperature was generally warmer with TABS, due to their slower heat extraction rate from the room. The findings are practical for analysing the design and operation of BHEs for different types of terminal units.

1. Introduction

Direct ground-cooling systems, also called geocooling systems, provide buildings with free cooling by circulating water through borehole heat exchangers (BHEs), i.e. an array of pipes inserted vertically into the ground [1]. Since BHEs are the only means of cooling the working fluid in the building cooling system, the sizing of BHEs is an extremely critical part of the system design. A system with BHEs that are too small is destined to decline in the cooling capacity in the long-term, as the outlet fluid temperature gradually exceeds the required limits. BHEs that are too large, on the other hand, incur excessive initial costs with no tangible outcomes for the system's thermal performance.

There are different approaches to sizing BHEs. One common approach is based on the borehole thermal analysis model by Eskilson [2], which was later adopted by Yavuzturk and Spitler [3] and Spitler [4] and has been implemented in design tools for commercial building ground heat exchangers, such as GLHEPRO [4] and EED [5]. This approach uses peak heating and cooling rates as well as monthly heating and cooling energies to size BHEs. In this approach, changes in annual ground temperature are determined by the total amount of heat injected into or extracted from the ground. On the other hand, the peak loads are used to determine the maximum or minimum borehole outlet fluid temperatures and they are presumed to have minimal influence on the long-term thermal performance of the BHEs. Therefore, minimising the peaks by controlling heat extraction rates from the space can significantly impact the sizing of BHEs.

Building terminal units based on the high-temperature cooling principle are functionally compatible with direct ground cooling systems, as they utilise high-temperature chilled water (>16 ℃) to cool spaces. From the heat exchange standpoint, high-temperature terminal units can generally be classified into radiant- and convective-based systems. TABS and chilled beams are examples of these terminal units, respectively.

The heat extraction rate from space is defined as the rate at which heat is removed from the space by means of a terminal unit. Terminal units have different heat extraction rates due to the differences in the heat transfer method (radiation vs. convection) [6–9] and/or their response time [10–13]. While beams and radiant ceiling panels are known as fast response systems, thermally activated building systems (TABS) are extremely slow, owing to a large

Abbreviations: ACB, Active chilled beam; BHE, Borehole heat exchanger; DGCS, Direct ground cooling system; PMV, Predicted mean vote; PPD, Predicted percentage dissatisfied; TABS, Thermally activated building systems.

* Corresponding author.
E-mail address: arghand@chalmers.se (T. Arghand).

https://doi.org/10.1016/j.enbuild.2021.110874
0378-7788/

structural thermal mass being involved in the thermal conditioning of the space [12].

Most of the previous studies on direct ground-coupled cooling systems were performed using slow response systems, such as floor/wall cooling systems [14–17] and TABS [18,19]. The main argument was the compatibility of these terminal units with borehole systems, as the ground could not tolerate fast and powerful peaks [20]. Only a few studies have evaluated the possibility of coupling the borehole systems with fast response terminal units, such as active chilled beams, fan-coil units and ceiling cooling panels [21–29]. The main focus in these studies was on the cooling performance and/or controllability of the system. The influence of heat extraction rates on sizing and dimensioning of the BHEs has not yet been extensively examined in the literature.

The key question we address in this study is how the sizing of BHEs is influenced by the type of building terminal units and their corresponding heat extraction rates. Two types of terminal units, namely active chilled beam (ACB) and TABS, are coupled to a direct ground cooling system. The simulation results for a single zone office present the cooling performance of the system on a daily basis and also during a cooling period.

2. Criteria for design and evaluation of the cooling systems

This study aims to investigate the design and sizing of BHEs in direct ground-coupled cooling systems (DGCSs) in relation to the terminal unit type. BHEs for DCGSs are basically designed to keep the borehole outlet temperature below a prescribed temperature throughout the cooling period. This study hypothesises that terminal units influence the sizing of BHEs by changing the peak hourly ground loads due to the differences in their heat extraction rates from the space. Therefore, to make a fair comparison, the total amount of heat injected into the ground during the cooling period is kept similar for all of the four cases studied. This is done by adjusting the design parameters of the terminal units, such as supply water temperature, water flow rate to the terminals and operation period of the cooling system. Keeping the amount of total heat injected into the ground similar for all cases is crucial because yearly ground temperature change is a function of the total heat injected into the ground. Peak cooling loads are different however, depending on the terminal unit type.

Another design aspect that is considered is that the ground-coupled system is thermally balanced, indicating that the annual heat injection into and extraction from the ground are equal. Therefore, the average annual ground temperature does not significantly change and hence, is not accounted for in the system design [26,30]. In order to cool the ground during the winter, water is circulated through a water-to-air heat exchanger in the air-handling unit to preheat the cold outdoor air. It is worth mentioning that an imbalanced system requires a much larger bore field to compensate for the ground temperature increase, otherwise the thermal performance of the system will gradually deteriorate.

Establishing a thermally comfortable indoor environment for occupants is the ultimate goal of building heating and cooling systems. Unlike stable indoor temperatures with ACBs, the indoor temperature in spaces handled by TABS change moderately during the occupied period [31]. Thus, the aim of designing TABS is to maintain thermal comfort within the acceptable range instead of keeping room temperature constant [32,33]. The thermal environment criteria considered in this study is to keep the highest room operative temperature below 26 ℃, equivalent to a predicted mean vote (PMV) of below + 0.5 on the thermal sensation scale and a predicted percentage dissatisfied (PPD) of below 10%, to fulfil category B for office buildings, according to ISO 7730 [34].

3. Simulation model

This study was performed using a simulation model of an office zone based on the experimental results from laboratory tests in a single office room. Fig. 1 shows the model development process. The process started by running experiments on a mock-up of a single office room (4.2 L × 3.0 W × 2.4H) equipped with a direct ground-coupled cooling system and an ACB (see Fig. 1A). Experiments in the office room were performed to investigate the hourly thermal performance of the ACB and the borehole system under variable heat gain conditions in the room. Based on the results obtained, a model of the room, the borehole system, the ACB and its operating systems were developed in the IDA ICE simulation tool and were validated against experimental data (see Fig. 1B). Fig. 1C shows the simulation model used in this study. The model is a modified arrangement of the validated model in larger dimensions. In addition, the warm window and floor in the validated model, which were used to simulate heat gain from solar radiation, were removed from the simulation model. Instead, windows were installed on the southern wall to simulate the external heat gain from solar radiation.

Readers are referred to our earlier article in [35] for a more detailed description of the experimental setup and conditions, measurement results, uncertainty analysis of the experiments, validation and accuracy of the simulation model, etc.

The simulated building is a single zone open-plan office equipped with a direct ground cooling system. The model includes the ground-coupled cooling system and the office zone. It was developed using the IDA-ICE version 4.8 building indoor climate and energy simulation tool. This software has been validated against the frameworks of various standards, including CIBSE TM33 [36], ANSI/ASHRAE 140 [37] and EN 13791[38].

3.1. Ground coupled cooling system

The cooling system includes the terminal units and the borehole system. The terminal units being investigated are ACB and TABS, each of which was being developed and being operated with two operating strategies. The borehole system consists of a single U-tube BHE. The following explains each part of the cooling system in detail.

3.1.1. TABS

TABS are water-based heating and cooling systems where pipes are embedded in a building's structural components, such as the floor or/and ceiling. Radiation is the main means of space heat extraction by TABS, but natural convection between TABS surface and room air also enhances the heat extraction rate. What distinguishes TABS from other radiant cooling terminal units is how it utilises the thermal mass of the building structure to buffer the sudden thermal loads. In fact, TABS stores heat and removes it later with respect to thermal loads [13].

A study by Nageler et al. [39] investigated the accuracy of the TABS model of IDA-ICE, and a strong correlation between the simulation results and the measurement data was found. In addition, IDA-ICE has also been used in other studies to evaluate the indoor thermal environment and/or the energy demand of buildings using TABS [40–42]. Appendix A provides a detailed description of TABS modelling in IDA ICE.

Fig. 2A is a schematic diagram of TABS used in this study. The pipes are embedded in a concrete slab 0.12 m below the floor surface. The thick insulation layer below the concrete slab minimises its thermal interaction with space below, indicating that TABS only removes heat from the upper side.

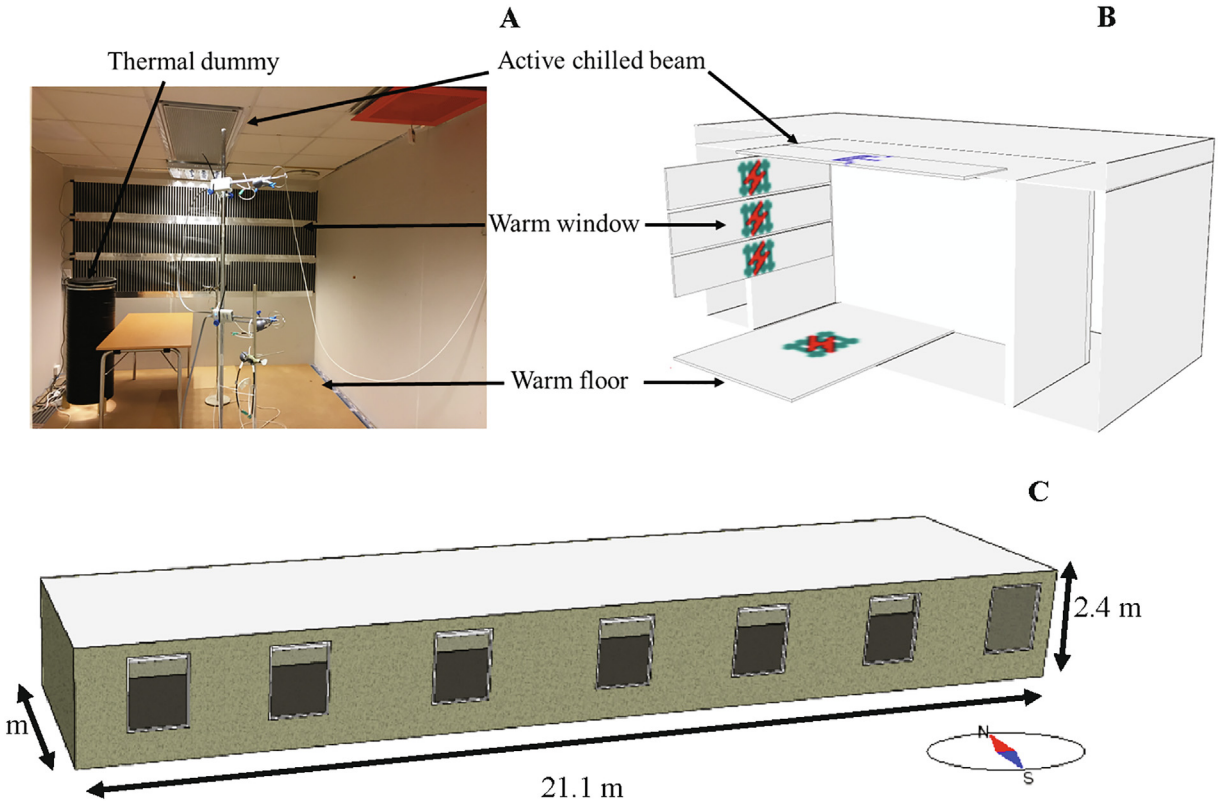

Fig. 1. A) Experimental facilities in a mock-up of an office room, B) simulated office in IDA ICE, and C) 3D modified office zone in IDA ICE.

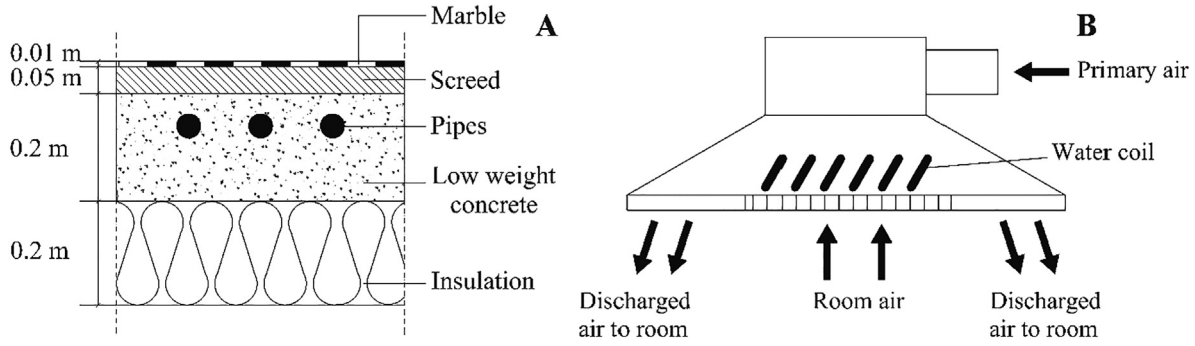

Fig. 2. Schematic layout of the terminal units studied A) TABS and B) active chilled beam.

The operating strategy for TABS was developed based on different operating schedules in combination with minimum room temperature control. Both operating strategies used in this study were among the common methods for controlling the TABS and were previously employed in other studies, including in [43–45]. However, they were modified to suit the requirements of this study. As stated in section 2, the common practice in designing TABS is to keep occupants' thermal comfort within the comfort condition instead of keeping the room temperature constant. Thus, the operating strategies are designed to keep the operative room temperature below 26 ℃ (PMV < 0.5 and PPD < 10%), corresponding to category B for office premises in ISO 7730 [46]. Room temperature levels in category B are aligned to the maximum allowed room operative temperature in offices according to the Swedish building regulations (BBR) [47], Swedish building owner association (BELOK) [48] and the Swedish work environment regulations (Arbetsmiljöverket) [49].

Fig. 3 shows the conceptual schematic of the heat extraction rates by operating strategies for TABS. TABS-A strategy operated the system intermittently with an interval of 1 h by switching the supply flow on or off. The switching time was supplemented with a feedback controller of the room operative temperature to avoid overcooling the room. The feedback controller stopped the flow anytime during the operation period if the room operative temperature fell below 22 ℃. The operating period of the system was 24 h for the workdays. The system also operated on Sundays from 15:00 to remove the accumulated heat in the space and avoid excessive heat injection into the ground when the system starts up on Monday mornings.

The TABS-B operating strategy was designed to keep the TABS surface temperature at about 22.6 ± 0.5 ℃. The operating strategy was implemented by supplying water at a constant temperature of 21.5 ℃ to TABS and the total flow rate alternated between 0.0 and 22.0 l/min (0–0.26 l/min.m^2) to adjust the surface temperature.

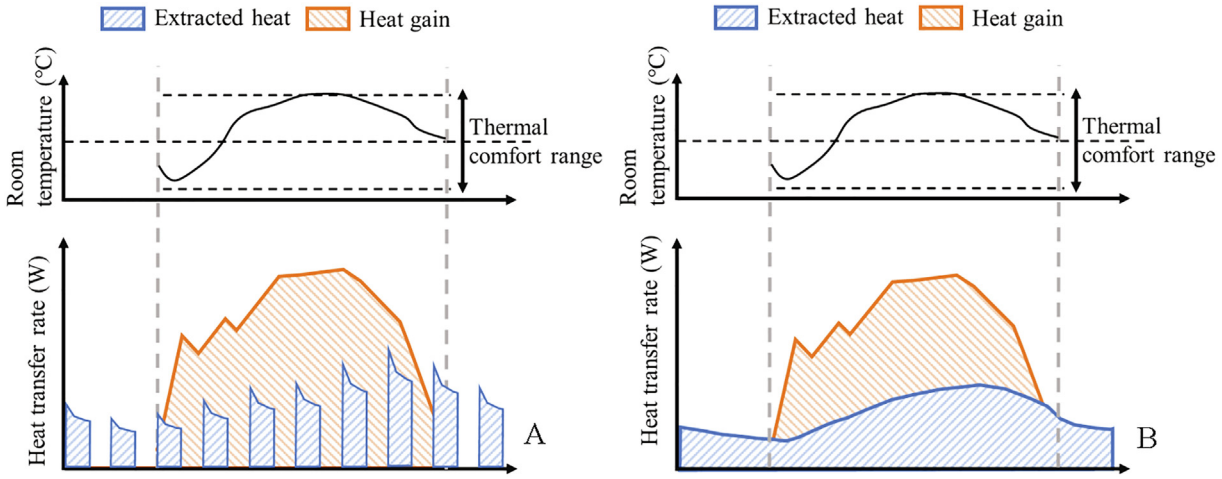

Fig. 3. Conceptual example of heat extraction rates by the operating strategies applied to TABS. A) Intermittent water flow rate to TABS (TABS-A) and B) Constant TABS surface temperature (TABS-B).

Table 1
Description of TABS input design parameters.

Structural parameters (unit)	
Floor area covered by TABS (m^2)	84.8
Total slab thickness (m)	0.46
Distance of pipes from the surface (m)	0.12
Pipes inner diameter (m)	0.01
Structural position (−)	Floor
Design parameters (unit)	
Supply water temperature (°C)	20.5 (TABS-A) 21.5 (TABS-B)
Supply water flow rate range (l/min)	0–22.0
Heat transfer coefficient from fluid to slab (W/m^2 K)	30

The operation schedule was similar to the TABS-A strategy. Table 1 summarises the main input design parameters for the TABS system.

3.1.2. Active chilled beams

IDA ICE simulates the ACBs as integrated convective-based terminal units comprised of hydronic and ventilation components (see Fig. 2B). The main cooling medium is water, but air also contributes to the thermal conditioning of the space if it is supplied at a temperature lower than room temperature. Input design parameters used in the model are summarised in Table 2. The nominal cooling capacity of the ACBs is 810 W under nominal air flow of 20 l/s, and supply and return water temperatures of 14 ℃ and 17 ℃, respectively. Appendix B gives a detailed description of the modelling of ACBs in IDA ICE.

Table 2
Description of the input design parameters of ACBs.

Number of ACBs (−)	7
Operation time period (−)	08:00–17:00
Nominal cooling capacity (W)	810
Primary airflow rate (l/s)	25
Exhaust airflow rate (l/s)	25
Primary air temperature (°C)	Room temperature
Supply water flow rate for each ACB (l/min)	5.6
Supply water temperature (°C)	16.0 (ACB-A operating strategy) 19.5 (ACB-B operating strategy)
ACB cooling capacity control method	On/off water flow (ACB-A operating strategy) Constant water supply temperature and flow rate to the beams (ACB-B operating strategy)

Two operating strategies were tested for the ACB system. The first method applied a feedback controller to keep the room temperature constant at the setpoint temperature (see Fig. 4A). The cooling capacity of the ACB was adjusted using an on/off controller to open and close a control valve connected to the beam.

The second operation strategy is implemented by supplying water to the ACB at a constant flow and a supply temperature close to the room temperature (≥20 ℃). The cooling capacity of the ACB is not regulated by means of a control system and the heat transfer between the ACB and space varies intrinsically with the room air temperature. In other words, changing the heat balance of the space results in room temperature change, which in turn changes the beam's heat extraction rate accordingly (see Fig. 4B). This is because the cooling capacity of ACBs is proportional to the difference between the mean water temperature in the coil and the room temperature. Using this method allows the room temperature to vary in response to changes in the room cooling load. This operation strategy is known as "self-regulating" and has previously been successfully used to operate ACB systems [26,50,51].

3.1.3. Borehole heat exchanger

The BHE was a closed-loop vertical single U-tube ground heat exchanger. The BHE was 200 m deep with a diameter of 110 mm. Ground thermal properties, undisturbed ground temperature and borehole thermal resistance were experimental data obtained by performing a thermal response test on a BHE drilled at the Chalmers University of Technology campus in Gothenburg, Sweden. The results were documented and reported by Javed [52]. Table 3 summarises the BHE design and thermal specifications.

BHE was modelled with an IDA-ICE single borehole model [53]. The borehole model has been validated against experimental measurements in our previous work [21]. The model considers radial and axial temperature fields around the BHE to calculate heat transfer within the BHE as well as between the BHE and the surrounding ground. Heat transfer calculations are done using a combination of the finite difference technique and the superposition method [53]. The model can perform transient heat transfer calculations to simulate heat conductivity and thermal capacity in the ground, temperature changes in the BHE fluid and thermal interactions between the BHE and the ground. The following heat transfer calculations are performed [54]:

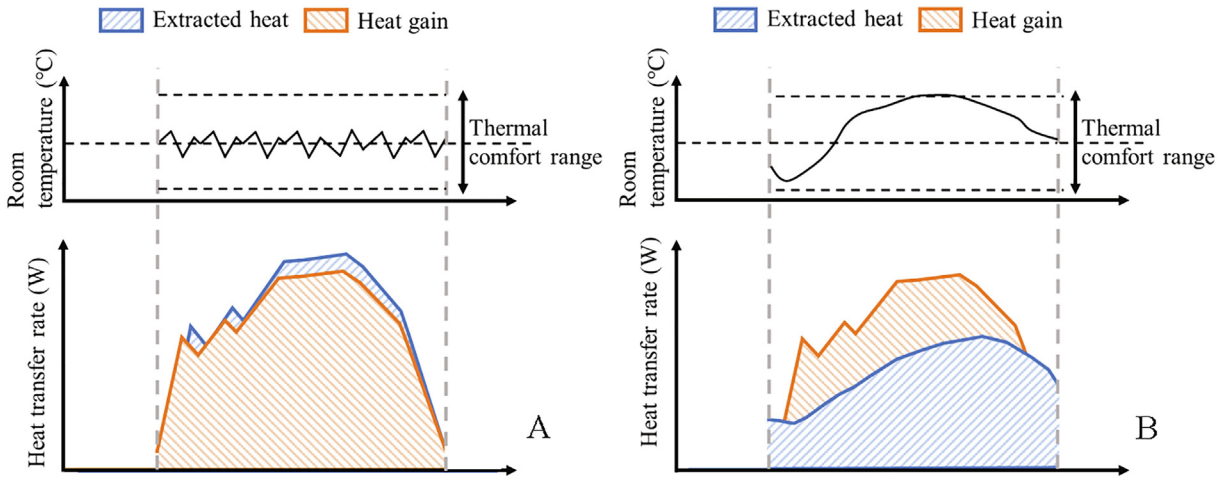

Fig. 4. Conceptual example of heat extraction rates by the operating strategies applied to ACBs. A) Typical feedback control method to keep the room temperature constant (ACB-A) and B) Variable room temperature operating strategy (ACB-B).

Table 3
Ground and BHE specifications.

Parameter (unit)	Specification
Ground	
Undisturbed ground temperature (°C)	8.3
Ground thermal conductivity (W/m K)	2.88
Borehole	
Total depth (m)	200
Diameter (mm)	110
Filling material	Ground water
Thermal resistance (m K/W)	0.059
U-tube	
U-tube type (−)	Single U-tube
Pipe type (−)	Polypropylene, PN8 DN40
Inner diameter (mm)	35.4
Outer diameter (mm)	40.0
Thermal conductivity (W/m K)	0.42
Circulating fluid	
Type	Ethanol (29.5%)
Thermal conductivity (W/m K)	0.401
Specific heat capacity (J/kg K)	4180
BHE fluid mass flow rate (kg/s)	0.5

- 1D heat transfer calculations for the inlet and outlet fluid in BHE along the U-tube's axial direction. The influence of fluid flow rate in the BHE is considered by taking the Reynolds number into account. It should be noted that the thermal mass of pipe material is neglected.
- 1D heat transfer calculations between the fluid, filling material and ground along the U-tube' radial direction.
- 2D heat transfer calculations between the BHE wall and the surrounding ground in cylindrical coordinates.

3.2. Office zone

Fig. 1C shows the office zone simulated in this study. The office zone was a south facing open-plan office with the area of 88.7 m^2. It had three external walls at the south, east and west. The southern wall was equipped with windows with a window to wall area ratio of 25% and no internal or external shadings. The northern wall and ceiling exchanged heat with internal spaces. The office zone was on the first floor and exchanged heat with the ground slab. The ground slab was part of the zone structure and behaved as a passive building component in the space heat transfer when ACB was operating. However, the slab was an active building component in cooling the space with the TABS systems. Input parameters of the zone model are summarised in Table 4. The simulated office was located in Gothenburg, Sweden, and the simulation period lasted from 14 May 2018 to 22 September 2018.

Space heat gain consists of external and internal gains, which are distinguished by their entry mode to the space. External heat gain was mainly generated by solar radiation from the windows installed on the southern wall, but also by conduction if the outdoor temperature was higher than the indoor temperature. Heat from people, lighting and equipment in the room made up the internal heat gain. Internal heat gain intensity was 18 W/m^2 and was active only during working hours (08:00–17:00) on weekdays.

3.3. Simulation method

Simulations of the DGCS were conducted in two time spans: daily and a cooling period of 4.5 months. Simulations on a daily basis sought to show differences in building peak hourly loads and room temperature given the operating strategies applied. Simulations of the system for the whole cooling period showed the distribution of the ground load and borehole outlet temperature, and how BHE sizing will be, considering the operating strategy and the

Table 4
Description of the input design parameters of the office zone.

Parameter (unit)	
External walls	
Dimensions (m)	21.1 W × 2.4 H (north and south) 4.2 W × 2.4 H (east and west)
U-value (W/m^2 K)	0.33
Thickness (m)	0.27
Internal walls	
Dimensions (m)	21.1 W × 2.4 H
U-value (W/m^2 K)	0.54
Thickness (m)	0.11
Windows	
Number of windows	7
Dimensions (m)	1.5 W × 1.2 H
Frame fraction (%)	10
U-value (W/m^2 K)	1.19
G-value (−)	0.43
Ground slab	
Dimensions (m)	21.1 L × 4.2 W
Thickness (m)	0.46
U-value (W/m^2 K)	0.14

terminal unit type. As previously stated, the total heat injected into the ground during the cooling period was similar for all case studies. However, the heat rejection rate into the ground is different, depending on the terminal unit type and/or operating strategy.

4. Results

The section describes the thermal performance of the cooling system on the peak cooling day as well as during the whole cooling period. Investigating the peak-hour loads is necessary for sizing all heating and cooling systems. However, sizing the ground coupled systems entails investigating the thermal loads throughout its operating period to consider the changes in the temperature and thermal storage effect of the ground.

4.1. Peak day

Figs. 5 and 6 show the hourly heat balance and room operative temperature of the simulated office on the design day. The design day was chosen because it represents the thermal performance of the cooling system under the peak condition. The results shown in the figures correspond to the peak cooling load conditions within the seasonal simulations. Total heat gain in the figures refers to the heat generated in the space from the internal and external sources. Heat extraction shows the heat removed by ACBs. Heat is only removed by the hydronic part of ACBs since the air is supplied at room temperature. Intensities of the total heat gain and heat extraction are different since part of the heat is transferred out of the space via internal/external building surfaces, and part of it becomes heat load in the space with a delay. The ground load is calculated based on the temperature difference between inlet and outlet borehole fluid.

The heat extraction rate in Fig. 5A shows a sudden increase at the start-up time because of the heat that accumulated in the space over the previous day. It then increases progressively and peaks at 4.49 kW. Heat extraction peaks approximately one hour after the peak of total heat gain, due to the buffering action of the room thermal mass. The ground load closely correlates with the heat extraction rate, indicating the capability of the BHE in providing

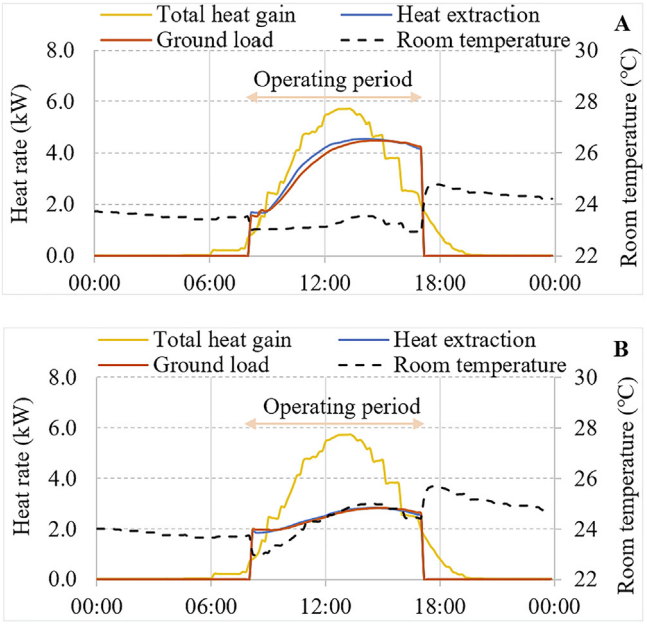

Fig. 5. Simulated heat flow rates and room operative temperature of the office cooled by ACBs with A) ACB-A operating strategy and B) ACB-B operating strategy.

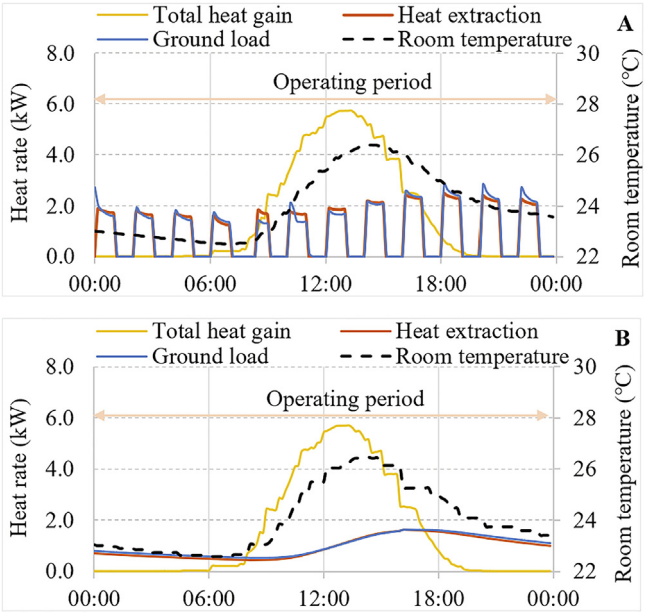

Fig. 6. Simulated heat flow rates and room operative temperature of the office cooled by TABS with A) TABS-A operating strategy and B) TABS-B operating strategy.

cooling water for the ACBs under the peak condition. In fact, Fig. 5A represents the thermal performance of a traditional feedback-controlled cooling system.

The heat extraction rate shown in Fig. 5B follows the same trend as that of room temperature. As previously explained in Section 3.1.2, the heat extraction rate of ACBs with the ACB-B operating strategy is directly associated with room temperature. The room temperature stays below 23.5 ℃ for approximately 2 h before the heat load of the space becomes greater than the heat extraction by the ACBs. It then gradually increases and causes the heat extraction rate to rise in a similar manner. Heat extraction peaks at about 2.84 kW at a room temperature of 25.0 ℃. A comparison of room temperatures and heat extraction peaks in Fig. 5A and Fig. 5B shows that applying the variable room temperature operating strategy caused the peak to reduce by 37%.

The ACB-A operating strategy provides a greater heat extraction rate for the beams thus resulting in lower accumulated heat in the building in comparison to the ACB-B operating strategy. Therefore, the room temperature with the ACB-B strategy is higher when the cooling system is switched off at 17:00. However, the accumulated heat is removed from the building at night-time in part due to the lower outdoor temperature (~10 ℃–15 ℃), and in part due to the building geometry. Consequently, the room temperature at the start-up of the system in the morning is not significantly different between the two cases.

Fig. 6 shows the heat flow rates and room temperature of the simulated office cooled by TABS on the design day. Heat extraction in Fig. 6A has an intermittent pattern, ranging between 2.48 kW and 1.55 kW, for the TABS-A operating strategy. For every operation cycle, heat extraction peaks at the start-up of the circulation pump, due to the high temperature difference between the supply and return water to and from TABS. Heat extraction gradually levels off after 20–30 min of operation. It can be seen that the system operates before and after the office hours, to remove the accumulated heat in the room.

Heat extraction with the TABS-B strategy shows a downward trend from midnight to 09:30, as shown in Fig. 6B. It then gradually increases to peak at 1.63 kW. The peak in heat extraction takes place approximately 3.5 h after the peak in the total heat gain.

Comparing TABS-A and TABS-B strategies, the heat extraction intensity is approximately 0.9 kW smaller with the TABS-B, because heat is extracted over a longer period. Nevertheless, the room operative temperature with both control strategies is similar because the same amount of heat is extracted from the space.

It is worth noting that the thermal mass of the floor influences the energy balance of the building differently depending on the terminal unit type. TABS actively involve the floor thermal mass in the heat transfer process. The cooled floor gradually absorbs heat from the space and rejects it to the working fluid in the pipes. On the contrary, the heat stored in the floor is rejected passively to the room when the ACB system is used. In this case, the floor only has a delaying effect by absorbing heat. Besides, less heat is absorbed by the floor as its temperature is close to the room temperature. If a thinner floor had been used in this study, a higher cooling capacity would have been required for ACBs.

4.2. Cooling period

The thermal performance of the cooling system was simulated between 14 May 2018 and 22 September 2018. The total heat injection into the ground during the cooling season was 1.64 ± 0.01 MWh and was similar for all cases investigated.

4.2.1. Ground loads

Fig. 7 shows ground load distribution during the cooling period in the form of boxplots. The ground loads are calculated based on the temperature difference between the inlet and outlet borehole fluid. Each central box of a boxplot presents the interquartile range, with a horizontal line at the median and the lower and the upper quartiles representing the 25th and 75th quartiles at the bottom and the top of each box. The whiskers define extra quartile values, with the dot symbols representing outliers, if any. It should be noted that the start-up ground loads for TABS on Sundays are excluded. This is because those loads are extremely intense, due to the amount of accumulated heat in the TABS, and considering them only causes the BHEs to be deeper without any tangible outcomes in comfort cooling, as the office is empty on Sundays.

Using the ACB operated with the ACB-A method causes the largest ground load compared to the other cases (see Fig. 7). This is because of the combined effect of using ACBs as terminal units and applying the constant room temperature control method. Compared to TABS, ACBs have a much faster dynamic performance in extracting heat from the space, resulting in a greater cooling demand. In addition, keeping a constant room temperature during the peak period has a consequence of increasing the cooling demand.

Comparing ACB-B with ACB-A strategies reveals the effectiveness of the operating strategy in reducing the heat injection rates into the ground. The peak decreased by 29%. The median and the 25th quartile with the ACB-B strategy are higher because it continuously operates the system even during low heat gain periods. The ACB-A strategy shuts the system during such conditions. It is interesting to note that the reduction in the peak load with ACB-B is significant so that the peak cooling demand of ACBs can even be comparable with TABS.

Ground loads with the TABS-A strategy are distributed over a larger range compared to TABS-B, due to the intermittent operation of the circulation pump. The ground load abruptly increases from zero to its maximum at the start-up of the pump when TABS-A operates the system because of a large temperature difference between the inlet and outlet BHE fluid temperatures. However, the TABS-B strategy runs the system continuously, which avoids having a large gradient between inlet and outlet fluid temperatures.

4.2.2. Outlet fluid temperature

Fig. 8 shows the borehole outlet temperature during the simulation period. As expected, the highest temperature in the outlet fluid appears for the ACB-A control method. Borehole outlet temperature increases during the peaks, owing to the slow heat transfer rate between the BHE and the surrounding ground. The ACB-A method has the greatest heat injection rate, resulting in the highest outlet fluid temperature.

Excluding the outliers from Fig. 8, the outlet temperature determined by the upper whisker falls within the 9.5 ℃ to 10.2 ℃ range for all cases. The likely explanation is that the BHE is sized based on the ACB-A method, which has the largest heat extraction rate. Therefore, the BHE is oversized for other cases and the differences in the space heat extraction rates do not make a significant change in the borehole outlet fluid temperature.

4.2.3. Room temperature

Comparing the system only from the BHE design point of view is rather one-sided. The goal of applying any heating and cooling systems in buildings is to satisfy the thermal sensation and comfort of the occupants. Local Swedish guidelines and regulations, such as the Arbetsmiljöverket [49] and the BBR [47], adopt similar

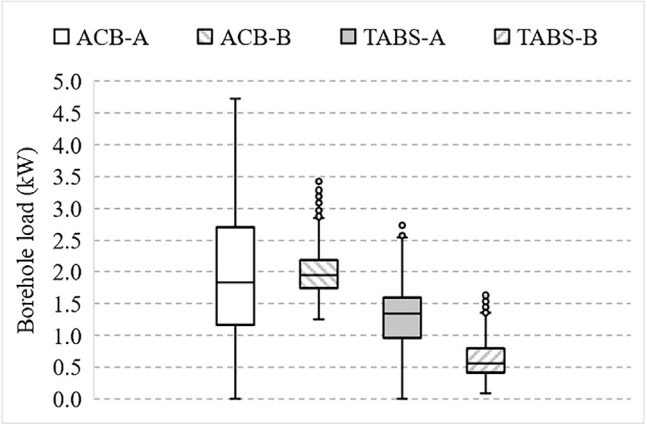

Fig. 7. Ground loads distribution for the cooling systems during the entire cooling period.

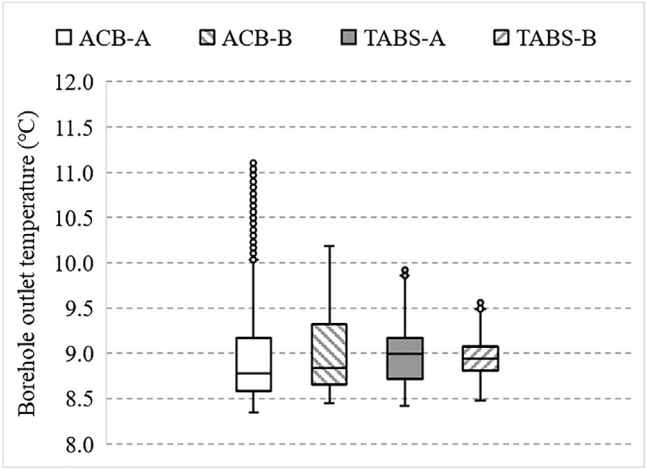

Fig. 8. Borehole outlet fluid temperature distribution. The undisturbed ground temperature is 8.3 ℃.

classifications to those suggested by ISO 7730 [46], wherein thermal comfort conditions of office buildings are classified using operative temperature. As stated previously in Section 2, the thermal comfort criterion followed in this study is to keep the operative temperature below 26 ℃, corresponding to a PMV of below + 0.5 on the thermal sensation scale.

Fig. 9 shows the upper operative temperature limits for comfort categories A and B according to ISO 7730 [46]. Room temperature is maintained within the comfort categories with all cases studied, but the distribution range is different.

The room temperature is well maintained around the setpoint temperature (23.0 ℃) with the ACB-A strategy. The values higher than the setpoint are due to the overshoot of the control system. Applying the ACB-B strategy reduces the heat extraction rate of the beams, which in turn, causes the room temperature to vary within a larger range, yet it fulfils category A requirements.

As expected, room operative temperature is distributed over a larger range with TABS compared to ACBs, since the cooling capacity and the heat extraction rate of TABS are lower. The maximum operative temperature achieved is only slightly above the upper limit (26 ℃). Further investigation shows that the number of overheating hours is only 4 h and 2 h for TABS-A and TABS-B strategies, respectively.

The operative temperatures shown in Fig. 9 are reproduced in Fig. 10 as duration curves, showing the cumulative duration for each cooling strategy. Results provided in this figure are practical for designing indoor temperature levels. For instance, the Swedish building owner association (BELOK) recommends room temperature levels between 21 ℃ and 26 ℃ and allows for overheating in office rooms for 80 h [48]. Maximum design temperature can therefore be 26.1 ℃, considering the overheating hours with TABS-B strategy. This means the room temperature will only surpass 24.9 ℃ for 80 h during the cooling period, which is acceptable. A similar comparison can be made for other terminal units and/or other room temperature levels.

4.3. Borehole size

In all the results presented so far, the BHE depth was 200 m. This depth is calculated based on the heat extraction rate of the ACB-A method to keep the fluid temperature leaving the borehole below 11 ℃. The resulting borehole provides the required cooling capacity to keep the room temperature at 23 ℃ with the ACB-A strategy. As shown in Sections 4.1 and 4.2.1, the operating strategy and the terminal unit type influence the heat injection rate into the ground, which in turn affects the outlet borehole fluid temperature.

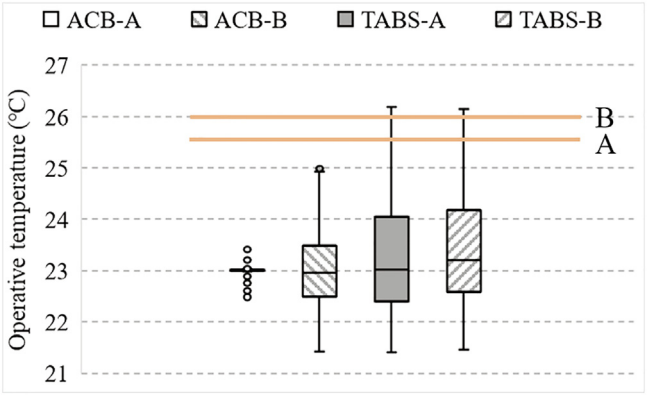

Fig. 9. Distribution of room operative temperature during the occupied hours (08:00–17:00) simulated for the whole cooling period. The horizontal line determine the upper limit of thermal comfort classifications A and B, according to ISO 7730 [44].

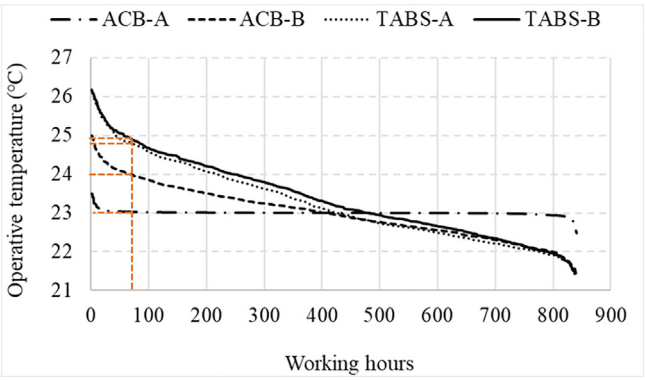

Fig. 10. Operative room temperature duration curves for the operating strategies tested.

In this section, BHE for each case is sized based on the actual heat injection into the ground shown in Fig. 8. The aim is to size the minimum BHE to provide a maximum outlet fluid temperature of 11 ℃ while maintaining the same room temperature and thermal comfort levels. Note that total heat rejection to the ground during the cooling period is still maintained at about 1.64 MWh for all cases. Thus, the calculated depth is influenced by the building peak loads, corresponding to the heat extraction rate from the terminal units.

Results shown in Fig. 11 can be discussed from the standpoint of terminal unit type and the operating strategy. Operating strategy has a great potential for reducing the BHE depth by reducing peak hourly loads. For instance, the variable operating strategy for ACBs effectively reduces the peak by increasing room temperature, and decreases maximum heat injection into the ground. The examined operating strategies for TABS can slightly change the peak intensity because TABS are slow-response terminals and changes in their hourly heat extraction rate do not happen rapidly.

Regarding the terminal unit type, using TABS instead of ACBs yields a shorter BHE and can reduce the depth by approximately 53% while meeting thermal comfort criteria. TABS extract heat from the space over a longer period. Thus, they reduce the peak intensity and prolong the period of heat injection into the ground. Both longer time and lower intensity are favourable to boreholes since boreholes also have slow thermal response behaviour. Nevertheless, if the design concerns having constant room temperature instead of keeping the thermal comfort criteria, a trade-off between higher room temperature and shorter BHE should be made for the design of the cooling system.

Another interesting point shown in Fig. 11 is the number of outliers in the outlet temperature for each case. Peak loads' intensity is directly proportional to the external heat gain from windows, and they cause the outlet temperature to increase on an hourly basis. A high number of outliers in the ACB-A outlet temperature compared to the other cases suggest its design is sensitive to the peaks. In fact, peaks extend the ACB-A outlet temperature by 1.1 K (from 10.0 ℃ to 11.1 ℃). This is stemmed from the fast heat removal rate by feedback-controlled ACBs. Applying the variable room temperature strategy reduces peak loads, which contributes to a significant decrease in BHE depth.

Another trade-off that needs to be considered when choosing a terminal unit is the pump energy use. Both the terminal unit type and the operating strategy influence the operation and the energy use of the circulation pumps. The energy use of the pumps in the ground loop and the building loop during the simulation period are computed to be 0.21 kWh/m^2 and 0.33 kWh/m^2 for the ACB-

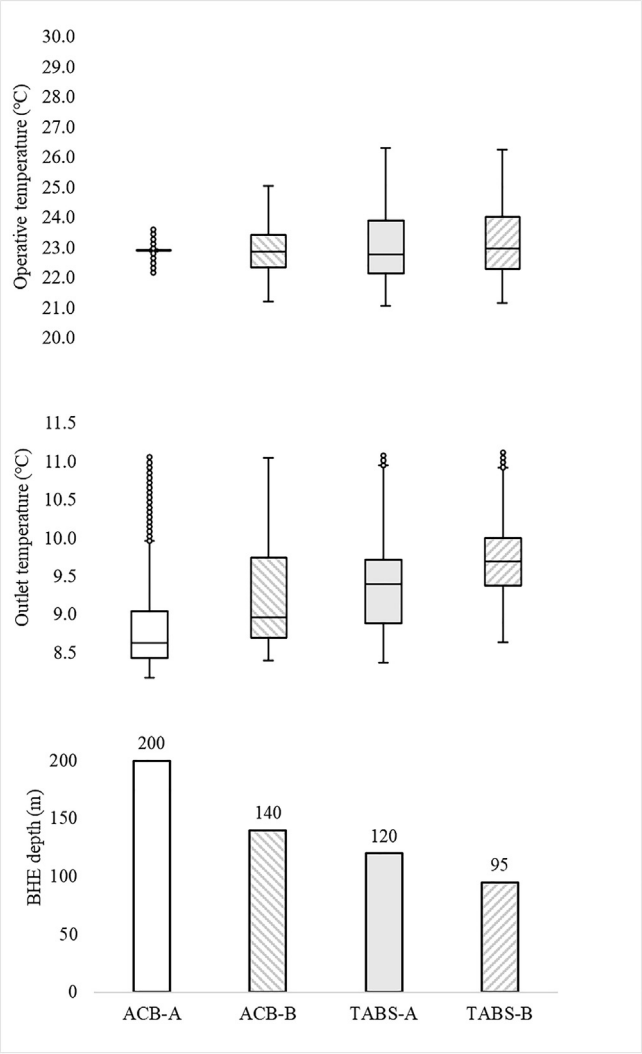

Fig. 11. Modified sizes of the BHE based on the actual heat injection rate from each terminal unit to the ground to obtain similar maximum outlet fluid temperature. The undisturbed ground temperature is 8.3 ℃ and total heat injection into the ground during the simulation period is similar for all cases.

A and ACB-B operating strategies, respectively. Lower pump energy use with the ACB-A strategy is associated with the intermittent flow control and the lower supply water temperature to the ACBs. The pump energy use for the operating strategies TABS-A and TABS-B are determined to be 0.36 kWh/m^2 and 0.76 kWh/m^2, respectively. The ground loop pump is operated continuously in the TABS-B strategy until the surface temperature falls below the setpoint temperature.

5. Discussion

In considering the results of this study, terminal unit type is found to be an influential parameter in sizing and dimensioning the BHEs, as the terminal unit type determines the heat extraction rates from the building and injection rates into the ground. Applying TABS can significantly reduce the size of the BHEs. TABS shave the building peak load by enlarging the heat extraction period and/or precooling the structural thermal mass. Importantly, our results show that slow response systems could allow the ground system to be much smaller than what would be required for fast-response systems to provide the space with the same amount of cooling energy. This issue was previously studied by Bourdakis et al. [55] for chiller-driven TABS and pipe-embedded systems. The findings of this study confirm the results previously reported in other studies regarding the compatibility of slow-response systems, such as TABS and pipe-embedded systems [16,20,56].

The degree to which the operating strategies can be effective in the design of BHEs depends on their influence in adjusting rates of heat extraction from the building and rates of heat injection into the ground. Applying variable room temperature control to ACBs successfully adjusted the cooling capacity of ACBs and reduced the peak by 29%. Our results comply with the findings reported in [15,57,58], indicating the influence of room temperature setpoint on the energy demand and peak intensity. However, the contribution of this article is the association of the influence of peak shaving with the sizing of BHEs. It is worth mentioning that the operating strategies applied to TABS in this study moderately influenced their heat extraction rates due to the limited cooling capacity of TABS. Applying other operating strategies, especially those using model predictive controls and weather forecasts, can change the heat extraction rates at peak conditions by adjusting the cooling capacity of the system in advance, as explained in [59–61].

To examine the question of which configuration of operating strategy and terminal unit best suits a direct ground cooling system, we shall consider both room thermal environment and BHE sizing requirements. Comfort categories A and B were met by all cases, although average room temperature was generally higher with TABS. The best choice seems to be taking BHE depth into account and using ACB operated with a variable room temperature method (ACB-B). Supplying water at a constant flow rate and temperature allows the terminal unit to extract heat as a function of temperature differences between the room and mean water temperature. Therefore, room temperature varies to make a balance between the cooling load in the room and heat extraction by the terminal without using zone control equipment. This control method was previously used for fast response terminal units, such as ceiling cooling panels by Arghand et al. [25] and ACBs by Filipsson et al. [26], Filipsson [62] and Kosonen and Penttinen [51].

Findings in this study denote the significance of using building simulation tools for designing direct ground coupled systems and avoiding rules-of-thumb or other simple calculation methods. Spitler and Cullin [63] pointed out that the long time constant of the ground and the highly variable relationship between peak loads and annual loads are two important parameters which make it nearly impossible for rules-of-thumb to estimate a right sizing range for BHEs. Given the results of this study, the dynamic performance of the building cooling system, including the terminal units and the control system, shall also be considered in the simulation process.

Finally, we suggest that thermal comfort requirements suggested in international and local standards for spaces with mechanical cooling should be regulated to leverage the advantages offered by direct ground cooling systems. One way is to consider certain overheating hours in the thermal comfort categories of the building. For instance, the Swedish building owner association, BELOK, suggests allowing 80 h of overheating of up to 26 ℃ in office buildings [48].

6. Conclusions

The influence of terminal units' type and the corresponding operating strategies on sizing BHEs in direct ground-cooling systems has been studied and quantified. Given the differences in thermal characteristics of the terminal units used, the evaluation criterion for the indoor thermal environment was to keep the room operative temperature below 26 ℃ (PMV < 0.6) to fulfil category B

in ISO 7730 for office buildings. In addition, to make a fair comparison for designing the BHE, the total amount of heat injected into the ground during the cooling period was equal in all cases studied. The following conclusions can be drawn:

- The heat extraction rate and response time of terminal units should be considered in the sizing and dimensioning of BHEs, as they highly influence the rates of heat injection into the ground. Using TABS instead of the traditional ACBs with feedback controllers (ACB-A operating strategy) reduced the peak hourly load by about 42–76%, depending on the operating strategy. However, the room temperature was generally higher with TABS.
- Considering a similar maximum borehole outlet temperature for all terminal unit types, applying TABS reduced the BHE depth by about 53% (from 200 m to 95 m) compared to a feedback-controlled ACB system.
- The variable room temperature operating strategy (ACB-B) demonstrated a significant potential for reducing the peak and therefore decreasing the rate of heat injection into the ground. Under the presumed simulation conditions, applying this method yielded approximately 30% BHE depth reductions (from 200 m to 140 m) compared to the traditional feedback control method.
- Considering both BHE depth and thermal comfort categories in the simulated office, ACBs operated by the variable room temperature method (ACB-B) demonstrated the best performance.
- The use of simplified sizing methods destines in either oversized or undersized BHEs since they usually overlook the actual heat injection/extraction rates into/from the ground.
- The choice of the terminal units must involve other considerations, e.g. embodied energy, operational energy and material use, life cycle costs and impacts, and installation, maintenance and replacement of these units. These aspects should be investigated in future studies.

Declaration of Competing Interest

The authors declare that they have no known competing financial interests or personal relationships that could have appeared to influence the work reported in this paper.

Acknowledgement

This work was financially supported by the Swedish Energy Agency (Energimyndigheten) through its E2B2 national research programme. The in-kind contribution of laboratory facilities by Swegon and Lindab is gratefully appreciated. We are particularly grateful to Håkan Larsson for his lab assistance. Valuable discussions with Carl-Ola Danielsson (Swegon) and Göran Hultmark (Lindab) are also acknowledged.

Appendix A

IDA-ICE heat transfer model for TABS consists of two components: the active component and the passive component. The active component includes the piping layer. The passive component simulates the heat transfer in the layers above and below the pipes. The model uses the supply temperature and the mass flow rate of water to calculate the return water temperature by using the logarithmic temperature difference between the mean fluid and the surrounding material, according to Eq. (1):

$$T_R = T_{Slab} + (T_S - T_{Slab}).e^{-\frac{h.A}{C_p.m_w}} \quad (1)$$

Where T_R is return water temperature (℃), T_{slab} is temperature of the heated layer (℃), T_S is supply water temperature (℃), h is the floor to slab heat transfer coefficient (W/m^2 K), A is the TABS (m^2) area, C_p is the specific cooling capacity of water (J/kg K) and $\dot{m}$ is the mass flow rate of water (kg/s).

For calculating the cooling capacity ($\dot{Q}$), the model assumes the active layer as an infinite conductive layer, indicating that the heat transfer between the active and the passive layer uses a 1D heat conduction model. Cooling capacity is calculated according to the steady-state resistance method given in EN 15377-1 [64] and EN 1264-5 [65]:

$$\dot{Q} = max(\frac{0.1}{c_p}, \dot{m_w}).c_p.(T_S - T_R) \quad (2)$$

Due to the boundary conditions assumed, the model needs to fulfil Eqs. (3) and (4) under steady-state conditions and Eq. (5) under transient conditions, according to EN 15377-1 [64].

$$\frac{S_i}{d_x} > 0.3 \quad (3)$$

$$\frac{d_a}{d_x} < 0.2 \quad (4)$$

$$\dot{m}_w.n.(R_w + R_r + R_x) \geq 0.5 \quad (5)$$

Where S_i is the thickness of the concrete slab from the outward edge of pipe to the slab surface (m), d_x is pipe spacing (m), d_a is the outer pipe diameter (m), n is the number of TABS sections, R_w is the thermal resistance between the fluid and the pipe wall (K/W), R_r is the thermal resistance through the pipe (K/W) and R_x is the thermal resistance between the pipes (K/W).

Appendix B

The ACB model in IDA ICE includes an idealised supply air terminal with a damper and a hydronic water coil heat exchanger [66]. The total thermal capacity ($\dot{Q}_t$) of an ACB is the sum of the capacity from the ventilation air ($\dot{Q}_a$) and the capacity of the hydronic water coil ($\dot{Q}_w$).

$$\dot{Q}_t = \dot{Q}_a + \dot{Q}_w \quad (6)$$

The cooling capacity of the water coil is a function of the temperature difference between the room air temperature and the water temperature running in the coil. It is calculated as [67]

$$\dot{Q}_w = K.\Delta T^n \quad (7)$$

$$\Delta T = T_{room} - \frac{T_S + T_R}{2} \quad (8)$$

where T_S is the supply water temperature, T_R (℃) is the return water temperature and T_{room} (℃) is the room air temperature. K and n are empirical factors associated with the primary air and water flow rates.

The cooling capacity of the air side is proportional to the temperature difference between the space's primary (T_p) and exhaust (T_e) air.

$$\dot{Q}_a = \dot{V}_a.\rho_a.c_{p,a}.(T_e - T_p) \quad (9)$$

where ρ_a (kg/m^3) and $C_{p,a}$ (J/kg K) are density and specific cooling capacity of air and $\dot{V}_a$ (m^3/s) is primary airflow rate to the beam. In this study, the temperature of the primary air to ACBs was adjusted to be equal to the room air temperature, similar to the laboratory setup. Therefore, the ventilation air had no contribution to

the thermal conditioning of the space and the heat was removed only by the water coil.

References

[1] D. Banks, An Introduction to Thermogeology: Ground Source Heating and Cooling, John Wiley & Sons, 2012.
[2] P. Eskilson, Thermal Analysis of Heat Extraction Boreholes PhD thesis, Department of Mathematical Physics, University of Lund, Lund, Sweden, 1987.
[3] C. Yavuzturk, J.D. Spitler, Short time step response factor model for vertical ground loop heat exchangers, ASHRAE Trans. 105 (1999) 475–485.
[4] J.D. Spitler, GLHEPRO-A design tool for commercial building ground loop heat exchangers, Proceedings for the Fourth International Heat Pumps in Cold Climates Conference. (2000) 1–15. http://www.hvac.okstate.edu/sites/default/files/pubs/papers/2000/08-HPCC_GLHEPRO.pdf.
[5] G. Hellström, B. Sanner, Earth Energy Designer: EED version 4, BLOCON Company, Lund, Sweden, 2020.
[6] J.(. Feng, S. Schiavon, F. Bauman, Cooling load differences between radiant and air systems, Energy Build. 65 (2013) 310–321, https://doi.org/10.1016/j.enbuild.2013.06.009.
[7] J. Woolley, S. Schiavon, F. Bauman, P. Raftery, J. Pantelic, Side-by-side laboratory comparison of space heat extraction rates and thermal energy use for radiant and all-air systems, Energy Build. 176 (2018) 139–150, https://doi.org/10.1016/j.enbuild.2018.06.018.
[8] J.(. Feng, F. Bauman, S. Schiavon, Experimental comparison of zone cooling load between radiant and air systems, Energy Build. 84 (2014) 152–159, https://doi.org/10.1016/j.enbuild.2014.07.080.
[9] J. Woolley, S. Schiavon, F. Bauman, P. Raftery, Side-by-side laboratory comparison of radiant and all-air cooling: How natural ventilation cooling and heat gain characteristics impact space heat extraction rates and daily thermal energy use, Energy Build. 200 (2019) 68–85, https://doi.org/10.1016/j.enbuild.2019.07.020.
[10] L. Berglund, R. Rascati, M.L. Markel, Radiant heating and control for comfort during transient conditions, ASHRAE Trans. 88 (1982) 765–775.
[11] ASHRAE, Radiant heating and cooling, in: ASHRAE Handbook—HVAC Systems and Equipment, American Society of Heating, Refrigerating and Air-conditioning Engineers, Atlanta, USA, 2016: pp. 6.1-6.21.
[12] B. Ning, S. Schiavon, F.S. Bauman, A novel classification scheme for design and control of radiant system based on thermal response time, Energy Build. 137 (2017) 38–45, https://doi.org/10.1016/j.enbuild.2016.12.013.
[13] J. Babiak, B.W. Olesen, D. Petras, Low Temperature Heating and High Temperature Cooling, Federation of European Heating, Ventilation and Air Conditioning Associations (REHVA), Brussels, Belgium, 2013.
[14] J. Romaní, L.F. Cabeza, P. Gabriel, A. Laura, A. De Gracia, Experimental testing of cooling internal loads with a radiant wall, Renewable Energy 116 (2018) 1–8, https://doi.org/10.1016/j.renene.2017.09.051.
[15] J. Romaní, G. Pérez, A. de Gracia, Experimental evaluation of a cooling radiant wall coupled to a ground heat exchanger, Energy Build. 129 (2016) 484–490, https://doi.org/10.1016/j.enbuild.2016.08.028.
[16] A. Li, X. Xu, Y. Sun, A study on pipe-embedded wall integrated with ground source-coupled heat exchanger for enhanced building energy efficiency in diverse climate regions, Energy Build. 121 (2016) 139–151, https://doi.org/10.1016/j.enbuild.2016.04.005.
[17] J. Liu, X. Xie, F. Qin, S. Song, D. Lv, A case study of ground source direct cooling system integrated with water storage tank system, Build. Simul. 9 (2016) 659–668, https://doi.org/10.1007/s12273-016-0297-0.
[18] K. Huchtemann, D. Müller, Combined simulation of a deep ground source heat exchanger and an office building, Build. Environ. 73 (2014) 97–105, https://doi.org/10.1016/j.buildenv.2013.12.003.
[19] S. Javed, I.R. Ørnes, M. Myrup, T.H. Dokka, Design optimization of the borehole system for a plus-Energy kindergarten in Oslo Norway, Archit. Eng. Des. Manage. 15 (2018) 181–195, https://doi.org/10.1080/17452007.2018.1555088.
[20] D. Pahud, M. Belliardi, P. Caputo, Geocooling potential of borehole heat exchangers' systems applied to low energy office buildings, Renewable Energy 45 (2012) 197–204, https://doi.org/10.1016/j.renene.2012.03.008.
[21] T. Arghand, S. Javed, A. Trüschel, J.O. Dalenbäck, Cooling of office buildings in cold climates using direct ground-coupled active chilled beams, Renewable Energy 164 (2021) 122–132, https://doi.org/10.1016/j.renene.2020.09.066.
[22] N. Deng, X. Yu, Y. Zhang, H. Ma, H. Wang, Numerical analysis of three direct cooling systems using underground energy storage: A case study of Jinghai County, Tianjin, China, Energy Build. 47 (2012) 612–618, https://doi.org/10.1016/j.enbuild.2011.12.038.
[23] Z. Li, W. Zhu, T. Bai, M. Zheng, Experimental study of a ground sink direct cooling system in cold areas, Energy Build. 41 (2009) 1233–1237, https://doi.org/10.1016/j.enbuild.2009.07.020.
[24] L. Liu, Z. Yu, H. Zhang, H. Yang, Performance improvements of a ground sink direct cooling system under intermittent operations, Energy Build. 116 (2016) 403–410, https://doi.org/10.1016/j.enbuild.2016.01.032.
[25] T. Arghand, S. Javed, A. Trüschel, J. Dalenbäck, Control methods for a direct-ground cooling system: An experimental study on office cooling with ground-coupled ceiling cooling panels, Energy Build. 197 (2019) 47–56, https://doi.org/10.1016/j.enbuild.2019.05.049.
[26] P. Filipsson, A. Trüschel, J. Gräslund, J.-O. Dalenbäck, Performance evaluation of a direct ground-coupled self-regulating active chilled beam system, Energy Build. 209 (2020) 109691, https://doi.org/10.1016/j.enbuild.2019.109691.
[27] T. Arghand, J.O. Dalenbäck, A. Trüschel, S. Javed, Some aspects of controlling radiant and convective cooling systems, in: 13th REHVA World Congress, E3S Web of Conferences, Bucharest, Romania, 2019. doi:10.1051/e3sconf/201911105008.
[28] Taha Arghand, Saqib Javed, Anders Trüschel, Jan-Olof Dalenbäck, Energy renovation strategies for office buildings using direct ground cooling systems, Sci. Tech. Built Environ. (2021), https://doi.org/10.1080/23744731.2021.1890520.
[29] Taha Arghand, Anders Trüschel, Jan-Olof Dalenbäck, Saqib Javed, Dynamic thermal performance and controllability of fan coil systems, 9th Cold Climate HVAC Conference (2018) 351–361, https://doi.org/10.1007/978-3-030-00662-4.
[30] H. Liu, H. Zhang, Performance Evaluation of Ground Heating and Cooling Systems- Long-term performance measurements of two case buildings, Department of Building and Environmental Technology, Lund University, Lund, Sweden, 2020.
[31] B.W. Olesen, Thermo active building systems: using building mass to heat and cool, ASHRAE J. 54 (2012) 44–52.
[32] CEN, EN 15377-3- Heating systems in buildings – Design of embedded water based surface heating and cooling systems – Part 3: Optimizing for use of renewable energy sources, European Committee for Standardization, Brussels, Belgium, 2007.
[33] ISO 11855-1: Building environment design – Design, dimensioning, installation and control of embedded radiant heating and cooling systems – Part 1: definition, symbols, and comfort area, European Committee for Standardization, Brussels, Belgium, 2018.
[34] CEN, EN 15251- Indoor environmental input parameters for design and assessment of energy performance of buildings addressing indoor air quality, thermal environment, lighting and acoustics, European Committee for Standardization, Brussels, Belgium, 2007.
[35] T. Arghand, S. Javed, A. Trüschel, J.-O.O. Dalenbäck, Influence of system operation on the design and performance of a direct groundcoupled cooling system, Energy Build. 234 (2021) 110709, https://doi.org/10.1016/j.enbuild.2020.110709.
[36] S. Moosberger, Report: IDA ICE CIBSE-Validation: test of IDA Indoor Climate and Energy version 4.0 according to CIBSE TM33, issue 3, Lucerne University of Applied Sciences and Arts, Luzern, Switzerland, 2007. http://www.equaonline.com/iceuser/validation/ICE-Validation-CIBSE_TM33.pdf.
[37] EQUA Simulation Technology Group, Technical report: Validation of IDA Indoor Climate and Energy 4.0 build 4 with respect to ANSI/ASHRAE Standard 140-2004, EQUA Simulation Technology Group, Stockholm, Sweden, 2010.
[38] S. Kropf, G. Zweifel, Validation of the Building Simulation Program IDA-ICE According to CEN 13791 "Thermal Performance of Buildings - Calculation of Internal Temperatures of a Room in Summer Without Mechanical Cooling - General Criteria and Validation Procedures", Lucerne University of Applied Sciences and Arts, Luzern, Switzerland, 2001.
[39] P. Nageler, G. Schweiger, M. Pichler, D. Brandl, T. Mach, R. Heimrath, H. Schranzhofer, C. Hochenauer, Validation of dynamic building energy simulation tools based on a real test-box with thermally activated building systems (TABS), Energy Build. 168 (2018) 42–55, https://doi.org/10.1016/j.enbuild.2018.03.025.
[40] B. Behrendt, Possibilities and Limitations of Thermally Activated Building Systems: Simply TABS and a Climate Classification for TABS, Technical University of Denmark (2016).
[41] G. Salvalai, J. Pfafferott, D. Jacob, Validation of a low-energy whole building simulation model, in: Fourth National Conference of IBPSA-USA, New York City, USA, 2010: pp. 32–39.
[42] J.; Babiak, G. Vagiannis, Thermally Activated Building System (TABS): Efficient cooling and heating of commercial buildings, in: 8th Mediterranean Congress of Heating, Ventilation and Air-Conditioning (CLIMAMED 15), Juan-les-Pins, France, 2015.
[43] D.O. Rijksen, C.J. Wisse, A.W.M. van Schijndel, Reducing peak requirements for cooling by using thermally activated building systems, Energy Build. 42 (2010) 298–304, https://doi.org/10.1016/j.enbuild.2009.09.007.
[44] B.W. Olesen, K. Sommer, B. Duchting, Control of slab heating and cooling systems studied by dynamic computer simulations, ASHRAE Trans. 108 (2002) 698.
[45] ISO, ISO 11855-6: Building environment design – Design, dimensioning, installation and control of embedded radiant heating and cooling systems – Part 6: Control, International Organization for Standardization, Geneva, Switzerland, 2012.
[46] ISO, ISO 7730- Ergonomics of the thermal environment – Analytical determination and interpretation of thermal comfort using calculation of the PMV and PPD indices and local thermal comfort criteria, International Organization for Standardization, Brussels, 2014.
[47] Boverket, Boverkeťs mandatory provisions and general recommendations, BBR, National Board of Housing (Boverket), Kalskrona, Sweden, 2018. https://www.boverket.se/en/start/publications/publications/2019/boverkets-building-regulations–mandatory-provisions-and-general-recommendations-bbr/.
[48] BELOK, Innemiljökrav för lokalbyggnader, The client group for premises (BELOK), Gothenburg, Sweden, 2015. http://belok.se/.

[49] Swedish Work Environment Authority, Workplace design- Provisions of the Swedish Work Environment Authority on workplace design (AFS 2009:2), Arbetsmiljöverket, Stockholm, Sweden, 2009. https://www.av.se/globalassets/filer/publikationer/foreskrifter/engelska/workplace-design-provisions-afs2009-2.pdf.
[50] Alessandro Maccarini, Göran Hultmark, Niels C. Bergsøe, Klemen Rupnik, Alireza Afshari, Field study of a self-regulating active beam system for simultaneous heating and cooling of office buildings, Energy Build. 224 (2020) 110223, https://doi.org/10.1016/j.enbuild.2020.110223.
[51] R. Kosonen, J. Penttinen, The effect of free cooling and demand-based ventilation on energy consumption of self-regulating and traditional chilled beam systems in cold climate, Indoor Built Environ. 26 (2017) 256–271, https://doi.org/10.1177/1420326X16683236.
[52] S. Javed, Design of ground source heat pump systems: Thermal modelling and evaluation of boreholes, Chalmers University of Technology, Gothenburg, Sweden, 2010.
[53] EQUA Simulation Technology Group, User Guide: Borehole 1.0, EQUA Simulation Technology Group, Stockholm, Sweden, 2014. http://www.equaonline.com/iceuser/pdf/UserGuideBoreholes.pdf.
[54] L. Eriksson, P. Skogqvist, Description of the IDA ICE borehole model, Internal Report, EQUA Simulation Technology Group, Stockholm, Sweden, 2017.
[55] E. Bourdakis, O.B. Kazanci, B.W. Olesen, Load calculations of radiant cooling systems for sizing the plant, Energy Procedia 78 (2015) 2639–2644, https://doi.org/10.1016/j.egypro.2015.11.333.
[56] M. Krzaczek, J. Florczuk, J. Tejchman, Improved energy management technique in pipe-embedded wall heating/cooling system in residential buildings, Appl. Energy 254 (2019) 113711, https://doi.org/10.1016/j.apenergy.2019.113711.
[57] G.N. Spyropoulos, C.A. Balaras, Energy consumption and the potential of energy savings in Hellenic office buildings used as bank branches – A case study, Energy Build. 43 (2011) 770–778, https://doi.org/10.1016/j.enbuild.2010.12.015.
[58] A. Baniasadi, D. Habibi, O. Bass, M.A.S. Masoum, Optimal real-time residential thermal energy management for peak-load shifting with experimental verification, IEEE Trans. Smart Grid 10 (2019) 5587–5599, https://doi.org/10.1109/TSG.2018.2887232.
[59] M. Gwerder, B. Lehmann, J. Tödtli, V. Dorer, F. Renggli, Control of thermally-activated building systems (TABS), Appl. Energy 85 (2008) 565–581, https://doi.org/10.1016/j.apenergy.2007.08.001.
[60] B. Lehmann, V. Dorer, M. Koschenz, Application range of thermally activated building systems tabs, Energy Build. 39 (2007) 593–598, https://doi.org/10.1016/j.enbuild.2006.09.009.
[61] C.D. Corbin, G.P. Henze, P. May-Ostendorp, A model predictive control optimization environment for real-time commercial building application, J. Build. Perform. Simul. 6 (2013) 159–174.
[62] P. Filipsson, Self-Regulating Active Chilled Beams, Chalmers University of Technology, Gothenburg, Sweden, 2020.
[63] J.D. Spitler, J.R. Cullin, Misconceptions Regarding Design of Ground-source Heat Pump Systems, in: World Renewable Energy Congress, Glasgow, Scotland, 2008.
[64] CEN, EN 15377-1- Heating systems in buildings – Design of embedded water based surface heating and cooling systems – Part 1: Determination of the design heating and cooling capacity, European Committee for Standardization, Brussels, Belgium, 2008.
[65] CEN, 1264-5- Water based surface embedded heating and cooling systems - Part 5: Heating and cooling surfaces embedded in floors, ceilings and walls - Determination of the thermal output, Part, Brussels, Belgium, 2008.
[66] EQUA Simulation Technology Group, User Manual- IDA Indoor Climate and Energy version 4.8, EQUA Simulation Technology Group, Stockholm, Sweden, 2018. http://www.equaonline.com/iceuser/pdf/ICE48GettingStartedEng.pdf.
[67] P. Filipsson, A. Trüschel, J. Gräslund, J.-O. Dalenbäck, A thermal model of an active chilled beam, Energy Build. 149 (2017) 83–90, https://doi.org/10.1016/j.enbuild.2017.05.032.